Electromagnetic Pulse Welding: Process Insights by High Speed Imaging and Numerical Simulation[*]

C. Pabst[1], P. Groche[1]

[1] Institute for Production Engineering and Forming Machines, TU Darmstadt, Germany

Abstract

Most researches on the mechanisms of impact welding in general base their results on the investigation of the joint area after the process, primarily by destructive testing. A detailed analysis of the joining process itself, especially concerning electromagnetic pulse welding, has not been performed yet and thus leads to a lack of understanding. As a consequence of this, the design of the joint area and the process parameters are almost exclusively found empirically.

With the help of a special image intensifier camera and a laser, which illuminates the joint area, a new attempt is made to visualize the impact in electromagnetic pulse welding. The results suggest that at least some mechanisms are currently not fully understood. Explanations are developed, mainly concerning jet formation (surface cleaning during the impact) and material behavior of the workpieces under the high strain rates of the process. Areas of large strain rates (liquid-like behavior of the metal) and areas of comparably small strain rates can be found within one workpiece. The question will be discussed whether process parameters can be gained with the help of a simulation that is sufficiently accurate at least in the macroscopic scale.

Keywords

Welding, impact, electromagnetic pulse welding, test rig

1   Introduction

Impact welding is a process which enables metallurgical bonds even between dissimilar metals. Explosion welding was the first practical implementation several decades ago. It uses the blast wave of powerful explosives and allows joining greater areas and thus is therefore mainly used for cladding. One important application is the production of vessels especially for the chemical industry, where high strength steels are combined with corrosion resistant metals, for example. A few decades later, electromagnetic pulse welding has been developed. It draws its energy from charged high voltage capacitors. The accelerating force on the workpiece is generated by a coil, through which the current is driven by discharging the capacitors. Compared to explosion welding, a much lower amount of energy is available and therefore only line-shaped joint areas can be achieved. However, it is safe and easy to conduct because no explosives are needed and the welds can be repeated in the range of seconds. Nowadays, the necessary coils and pulse generators meet the industrially requested lifetimes. The main applications of electromagnetic pulse welding are the construction of hybrid space frames, the gas-tight sealing of high pressure containers or low-ohmic joints between aluminum to copper for the electromobility. The joints produced with impact welding are very tough, because the joint area is not weakened by thermal influences but exhibits fine grains [1].

Despite all advantages of impact welding in general and of electromagnetic pulse welding in particular, the latter is still not widely spread. One reason is the comparably poor predictability of the weld, which requires an empirical design of the joint area and the machine setup. The investigation of the process principles is challenging: Explosion welding is a stationary process, but requires large amounts of explosives and is therefore hard to observe. Electromagnetic pulse welding can be easily observed, but the impact parameters constantly change during the collision [2].

The basic mechanisms are understood [3,4] and illustrated in Figure 1: One workpiece has to impact another at velocities (v_{imp}) in the range of roughly about 250 m/s and above. The impact has to occur under a certain impact angle (β_{imp}). This leads to a collision point (or line) travelling across the surface.
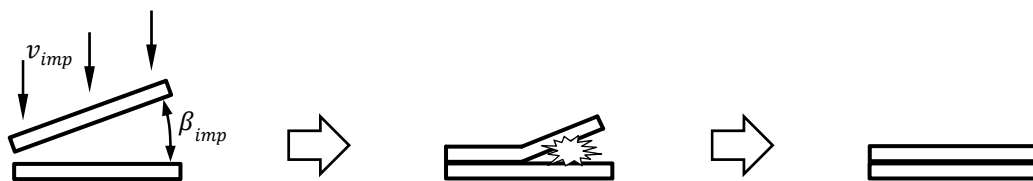

Figure 1: Schematic illustration of impact welding.

Due to the high strains and strain rates in this area, superficial oxides and impurities are removed and driven out of the closing gap. The impact is accompanied by a bright flash which is characteristic for this process. The metallically pure surfaces are then pressed together by the immense pressure of the impact, which finally evokes the metallurgical joint. [5]

2   Experimental Setup

For the basic investigations, a special test rig has been developed at the PtU. It avoids the drawbacks of explosion welding and electromagnetic pulse welding by colliding and welding flat sheets mechanically. The buildup consists of two rotors which are driven by one synchronous motor each. Each rotor holds an aluminum tube with a length of 500 mm. At one end of each rotor a welding specimen is mounted and a counterweight is attached to the opposite side. Figure 2 shows the test rig without housing.
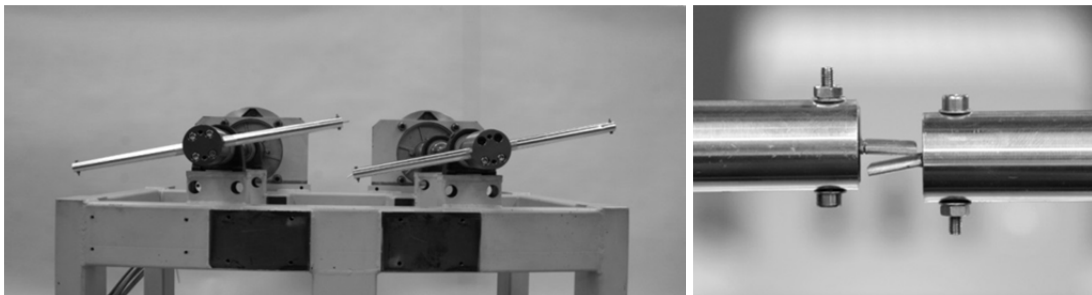

Figure 2: Left: Test rig without housing. Right: Rotors with specimens in collision position.

Both rotors have the same sense of rotation, so the specimens' velocity adds when they meet in the center. The maximum speed of 6000 rpm equals an impact speed of about 300 m/s. Further improvements are planned in order to increase the collision speed by greater lengths of the aluminum tubes. When the specimens are welded successfully, they rip off their clamped rest with the help of a predetermined breaking point. The welded specimens (EN-AW1050A) and the clamped parts are shown in Figure 3.

Figure 3: Welded specimens (center) with the clamped parts.

The test rig allows to set the initial impact angle (β_{imp}) and the initial impact velocity (v_{imp}) independently. The latter is independent of the specimens' mass in contrast to explosion welding or electromagnetic pulse welding. To adjust the desired impact angle, one specimen is bent correspondingly (right image in Figure 2). The test rig has proven its capabilities in first results, which are described in [2] in more detail.

3   Numerical Simulation

As motivated above, one aim is to be able to predict the necessary process parameters and, with the help of this knowledge, the extent of the actual metallurgically joined area. This allows to find the ideal design for the joint area and to achieve the best possible weld during the development of the products without costly experimental parameter studies. One of the greatest challenges here are the high strain rates of the impact welding processes: Directly at the bond area, strain rates are in the order of magnitude of 10^5-10^7 1/s. At these high strain rates, metals show a liquid-like behavior without being actually molten. A result of this is the wavy interface of the weld and the emission of superficial impurities as the so-called jet. If the small weld area is to be simulated, the material model has to be able to represent these properties. Material models like for example Steinberg-Lund or Zerilli-Armstrong are suitable for this task. In addition, the contact definition and the discretization have to be chosen correspondingly. In [6], for example, the Smooth Particle Hydrodynamics method (SPH) has been used to model the joint formation. Both the jet and the wavy interface have been simulated successfully by applying a hybrid mesh consisting of Lagrange elements for the base material and the SPH method for the actual impact area. This procedure provided good results but at the same time exhibits two disadvantages: It is quite complex and the necessary parameters for the material model at very high strain rates are required. The latter are difficult to obtain and therefore very expensive. Hence it would be very advantageous if the weld could be predicted without the need for a detailed simulation in a microscopic scale.

Therefore the aim of the numerical simulation in this paper is to investigate whether it can be sufficient to model the impact process in a macroscopic scale. Process windows are known from explosion welding, which depend on the angle β directly at the collision point and its velocity v_c. Figure 4 shows both quantities and a qualitative process window. It can be easily seen that impact velocity v_{imp} and impact angle β_{imp} are not equal to v_c and β, respectively. All angles and velocities are macroscopically visible and thus should be easy to observe and to simulate.
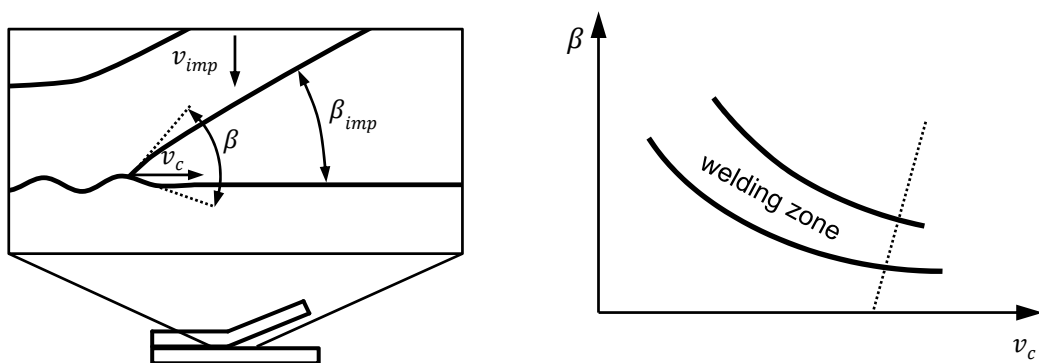

Figure 4: Left: Angles and velocities close to the collision point. Right: Qualitative process window derived from explosion welding.

The thickness of the jet and the amplitude of the wavy interface are small compared to the other dimensions. Consequently, it appears possible to neglect their influence on both angle and velocity. In doing so, element size can be increased and the maximum

strain rates are lower, because the areas of large strain rates (and strains) are just one small part of an element. Thus, computation time is reduced and the material definition can be simplified.

In this paper a simplified and two-dimensional geometry is used for the simulation which represents the collision in the test rig. It consists of two sheets with a thickness of 2 mm and a length of 10 mm approaching each other. The angle and the velocity are set independently. The simplified Johnson-Cook material model is used with the parameters for EN-AW1050A A = 140 N/mm², B = 75 N/mm², n = 0.65 and C = 0.0125. The calculation is carried out with a solver of LS-DYNA. Figure 5 shows the setup of the simulation and its evaluation. The coordinates of the superficial nodes on the opposing faces are analyzed and the angle β at and the velocity v_c of the collision point are calculated for each time step by an additional script in Matlab. A more detailed description of this procedure and the estimated process window can be found in [2].
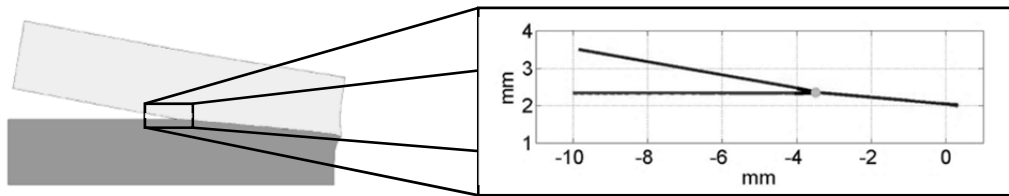

Figure 5: Left: Setup of the simulation. Right: Evaluation of angle β and velocity v_c as seen by the script running in Matlab.

Irrespective of the simplification, the question arises whether material properties have a great influence on the results. Due to the great dynamic of the impact process it could be expected that the material density has a significant effect on the deformation behavior. To check this assumption, each of the parameters of the Johnson-Cook material model (A, B, n and C) is varied by 40 % in positive and negative direction which equals the factors 0.6 and 1.4, respectively. For example Parameter A, which is 140 N/mm² by default, is set to 84 N/mm² and 196 N/mm². The result is a fictional material. The following Figure 6 shows the results for the collision point angle β versus the collision point velocity v_c for a variation of all four parameters. The impact angle β_{imp} is always set to 10° and the normal impact velocity v_{imp} of each sheet is always set to 125 m/s, which equals 5000 rpm of the test rig. Starting with A, it is quite obvious that it has a great influence on the impact angle β. The parameters B and n only have a minor effect on the result as well as the parameter C. An attempt can be made regarding the governing formula developed by Johnson and Cook [7]:

$$\sigma = \left(A + B\,\epsilon_p^n\right)(1 + C\,ln\dot{\epsilon}) \qquad (1)$$

ϵ_p and $\dot{\epsilon}$ denote the effective plastic strain and the (normalized) strain rate, respectively. B and n determine the influence on the plastic strain which explains the negligible effect on the results: The maximum plastic strain at the impact area is even below 0.5. The low sensitivity to parameter C is surprising at first glance, because it is directly linked to the (plastic) strain rate. However, it can be easily explained by the logarithm which weakens the effect of even the high strain rates.
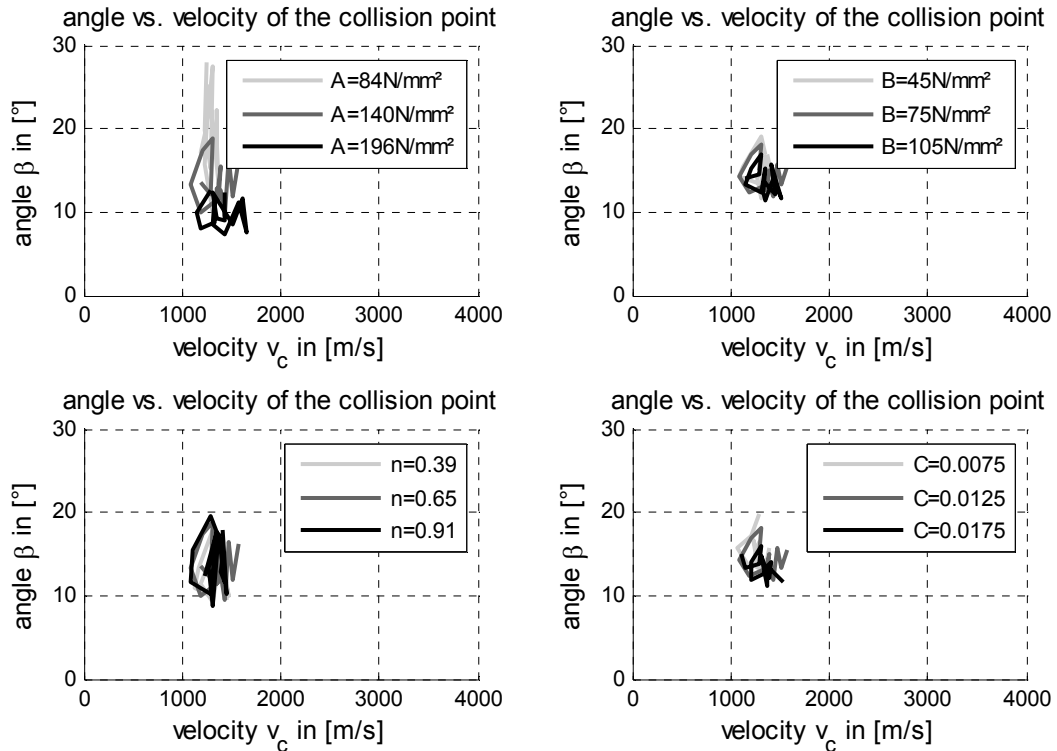
Figure 6: Collision angle versus collision point velocity for different sets of material model parameters (left to right, top to bottom : A, B, n, C).

The material density is varied next, again by adding and subtracting 40 %, respectively. The resultant plot is given in Figure 7 (left). As assumed above it is clearly visible that the density of the colliding joining partners has a great effect on the results, mainly on the impact angle. Preliminary to a detailed discussion, the calculation will be extended to the variation of the impact velocity of both parts. Although a much lower deviation of ± 20 % is chosen, both angle β and velocity v_c are significantly shifted to higher values. The resultant plot is shown in Figure 7 (right).
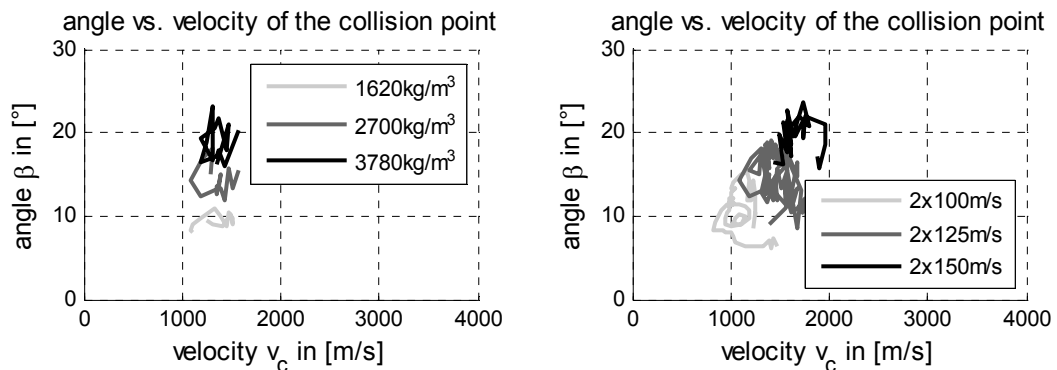

Figure 7: Collision angle versus collision point velocity for three different material densities (left) and three normal impact velocities (right).

Comparing the plots for different densities and for different velocities, a common trend becomes obvious: Higher velocities and higher densities lead to higher angles. This effect is plausible as an increase of the speed and/or the angle is equivalent to an increase in kinetic energy. This kinetic energy in turn depends on the impact velocity and the mass (density). The exact reason for the increasing angle might be some kind of a "whip effect" during the impact. The increasing collision point velocity, when increasing the impact velocity, may be caused by the geometric constraints: Ignoring the deformation of both joining partners and with regard to the geometric constellation depicted in Figure 4, the collision point velocity can be estimated by

$$v_c = \frac{v_{imp}}{\tan \beta_{imp}}. \tag{2}$$

A similar behavior can be observed in simulations of electromagnetic pulse welding. The calculated setup involves two aluminum sheets with a thickness of 2 mm and an initial distance of 2 mm. The current is driven through a nearby coil at a frequency of 20 kHz. A more detailed description on this numerical setup and the electromagnetic simulation can be found in [2]. The evaluation of the results for different maximum currents (Figure 8) shows that higher currents and thus higher impact speeds lead to higher angles and velocities as well, especially at the end of the process (left half).
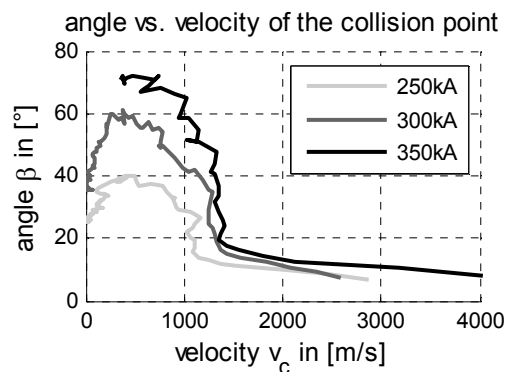
angle vs. velocity of the collision point

Figure 8: Collision angle versus collision point velocity for three different peak currents.

4 High Speed Imaging

As the actual impact and the joint formation take place in only few microseconds, the process is hard to capture with a conventional high speed camera. Hence for these research works, an image intensifier camera is used. It allows exposure times and frame delays in the range of nanoseconds at still remarkable spatial resolutions of up to more than 1000 pixels.

Filming the impact is accompanied by two more obstacles in addition to the high speeds: During the impact, a bright flash covers the actual joint area. Its formation will be discussed in the following chapter. Exact triggering is the second challenge, because the camera technique does not allow pre-triggering. Due to the fast turning rotors, the exact measurement of the momentary angle is hardly possible.

The bright process glare can be suppressed by a trick which is also used when conventional welding processes are investigated. As the glare is usually whitely, it can be concluded that its intensity is spread almost constantly across all (visible) wavelengths. The light source which is mandatory for the high speed images only emits light in a small wavelength range. Thus, its intensity is much greater than the process glare, even if the latter appears to be brighter to the human eye. Figure 9 illustrates this issue.
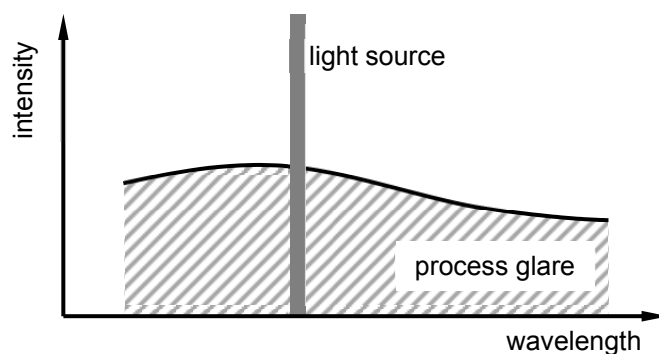

Figure 9: Emitted wavelength range of the light source and the wavelength distribution of the process light.

To suppress all other wavelengths, an optical bandpass filter is fitted to the camera in addition to the special light source. In the experiments, a laser with a nominal wavelength of 640 nm ± 10 nm is used together with a filter for 640 nm ± 5 nm. The laser is comparably easy to handle, because the light is visible and the emitted beam itself is neither coherent nor collimated. This avoids speckling and makes reflections harmless even despite the power of 400 W. The laser pulses are synchronized with the camera, because their length is limited to a few microseconds only due to the limited duty cycle which prevents a constant illumination.

Triggering is realized by using the two rotors as a kind of switch for the trigger circuit. A voltage is applied to one rotor whereas the other rotor is connected to ground. In addition, each rotor is mounted electrically insulated from the test rig's framework. When the specimens collide, the circuit is closed and a voltage signal is generated which can be directly used as trigger signal. This system is very robust and even works if the specimens do not collide exactly at the center.

The following Figure 10 shows the process in two independent experiments immediately after the finished impact with and without bandpass filter. It can be clearly seen that it is almost impossible to investigate the impact in detail without the filter.
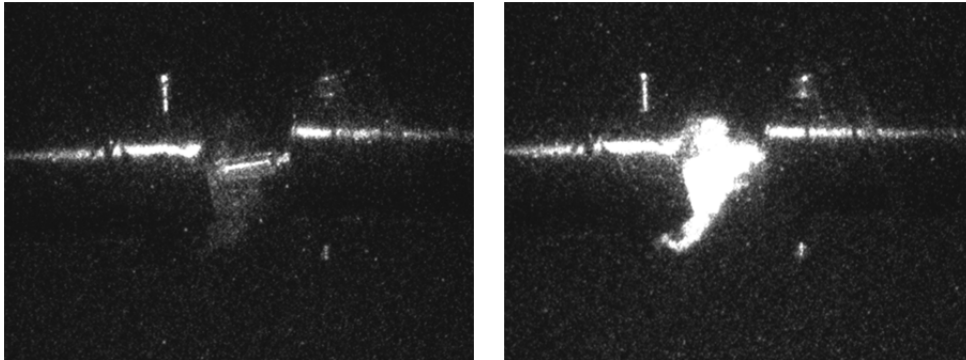

Figure 10: Propagation of the jet 20 µs after the impact with (left) and without (right) optical bandpass filter.

5   Jet Formation and Process Glare

A common explanation for the process glare is that it is caused by the jet. The jet does not only consist of oxides, but also of parent material [6]. The theory states that this parent material burns whilst being emitted and thus causes the intense light. However, it is generally accepted at the same time that high temperatures or even melting do not occur during the impact and welding process. Thus, a sufficient energy source which is capable of initiating the oxidation should actually not exist.

In order to examine jetting and glare in more detail, the electromagnetic pulse welding process is investigated under different atmospheres. It is more convenient than the test rig because only the small volume around the tool coil has to be filled with the respective gas. The complete housing of the test rig has a volume of approximately 1 m³ and is not gas-tight. For the experiments, the coil is covered by an acrylic glass box, which is filled with an inert welding gas. It consists of argon and about 8 % CO_2 which makes the inert gas heavier than the surrounding air and therefore simplifies its displacement. When the enclosure is completely filled with the inert gas, the pulse generator is charged and the weld is established after only few seconds. The following images show the welding of two aluminum sheets (EN-AW1050A) with a thickness of 2 mm by a peak current of 300 kA at 20 kHz. Figure 11 shows the welding process with the inert gas atmosphere (left) and with the surrounding air (right). The inert gas does not only significantly decrease the emitted light, but also strongly weakens the emitted pressure wave during the impact.
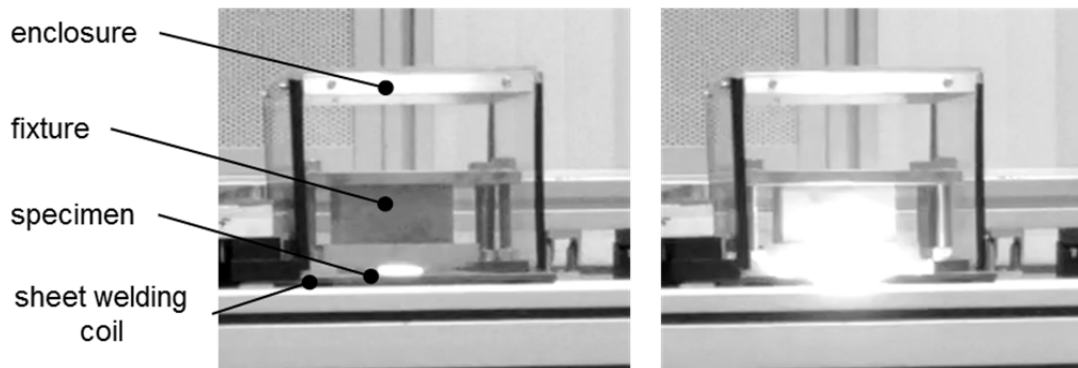
Figure 11: Electromagnetic pulse welding of two aluminum sheets with (left) and without (right) inert gas atmosphere.

Welds between two copper sheets (Cu-ETP, thickness 1 mm) show a different behavior: Neither the light emission nor the pressure wave is significantly influenced by the surrounding atmosphere. In both cases, it is comparable to aluminum welds with inert gas.

These experimental results suggest that an oxidation proceeds during the impact. Aluminum burns with a bright white flame and the oxidation is a highly exothermal reaction. As it can be seen in Figure 10, the emitted jet looks like a cloud of dust. If this dust does not only consist of superficial oxides but also of pure aluminum from the base material, which has been proven in past researches [6], a huge surface is created. Thus, if an appropriate energy source is available, a strong exothermal reaction can occur. This theory is supported by the experiments with the test rig: The extent of the glare and the extent of the jet are almost identical as highlighted in Figure 12. This indicates that jetting and glare are the same phenomenon or at least correlate closely.
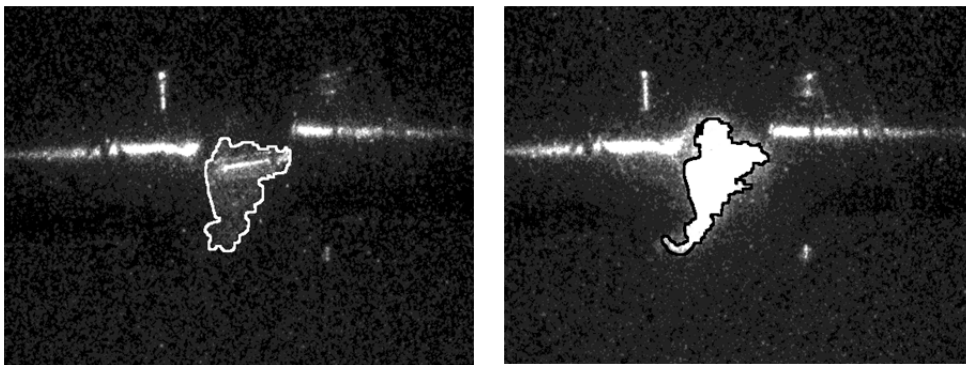

Figure 12: Highlighted propagation of the jet, with (left) and without (right) optical bandpass filter.

The auto ignition temperature of aluminum strongly depends on the particle size. The past research work in this field, which has been summarized in [8], shows that the auto ignition of aluminum powder with a particle size of under 10 μm can already happen at about 600 °C. As burning aluminum is even capable of splitting water molecules, a hydrogen explosion due to the atmospheric humidity might occur as well. Copper on the other hand does not burn, which explains why the surrounding atmosphere does not change the light emission.

Nevertheless, the question arises where the necessary temperature for the ignition is created. Two theories appear imaginable:

1. During the impact, temperatures reach higher values than generally assumed. Temperatures of several hundred degrees Celsius are possible and thus are capable of igniting the jet.
2. During the movement of the collision point, which travels at a multiple speed of sound, its supersonic pressure wave generates a plasma which in turn ignites the jet.

The first approach is supported by the welding trials with an inert gas atmosphere. A small luminous effect can be observed even though an oxidation can be excluded. This could imply that temperatures are reached which are even sufficient to heat up copper until it glows. This again might lead to molten areas, which actually should not occur in impact welding as a solid state welding process. However, studies have revealed that a thin intermetallic layer can be observed at least in dissimilar metal combinations [9]. Furthermore, the ultra-fine grains could be caused by a very fast melting and solidifying process. This appears possible as the molten area is very small and very rapidly cooled down by the surrounding material, because metals usually exhibit a good thermal conductivity.

The second approach relies on the minor radiance as well. Immediately after the first contact, the collision point travels at very high velocities along the surfaces (right half in Figure 8) and pushes the surrounding gas out of the closing gap. Due to the high velocity, which can reach more than ten times the speed of sound, a powerful shock wave is generated. The energy of this shock wave could be sufficient to create a plasma from the ambient gases. The plasma temperature is high enough to ignite the jet which can then be observed as a bright flash if oxygen is available.

6 Summary

The experimental setup which enables the investigation of the impact welding process in a secure way and under clearly defined conditions has been presented. The numerical approximation of the impact has been described and the results from a parameter study have been discussed. It has been shown that inertia seems to play an important role. A promising method to observe the actual welding process by high speed imaging has been presented and first images have been discussed. They enable the closer investigation of the welding zone. Experiments have been conducted to find out more about the jet formation and the process glare. Two theories have been developed and discussed. They will be closely investigated in the future.

7 Conclusion and Outlook on Future Works

The numerical simulation of the impact in a macroscopic scale provides plausible results, even though it is kept very simple. Even the influence of the breaking point of the specimens remains disregarded. Future experiments and high speed images will show whether this simplification is justified or not. It appears possible to give analytic explanations to the numerical results

The test rig will be steadily improved in order to achieve higher impact speeds under more exact impact conditions.

The high speed images will be helpful in investigating the formation of the jet the glare during the impact. By using a higher magnification and a higher frame rate, the identification of the origin of both the jet and the glare should be possible. This will prove whether one of the theories applies or not.

References

[1] *Zhang, Y.; Babu, S.; Daehn, S.:* Impact Welding in a Variety of Geometric Configurations. In: 4th International Conference on High Speed Forming, 2010, pp. 97-107

[2] *Groche, P.; Wagner, M. F.-X.; Pabst, C.; Sharafiev, S.:* Development of a novel test rig to investigate the fundamentals of impact welding. In: Journal of Materials Processing Technology. 2013. http://dx.doi.org/10.1016/j.jmatprotec.2013.10.008

[3] *Carpenter, S.H.; Wittman, R.H.:* Explosion Welding. In: Annual Review of Materials Science, pp. 177-199, 1975

[4] *Crossland, B.:* Explosive Welding of Metals and Its Applications. In: Oxford Series on Advanced Manufacturing, Clarendon Press, Oxford, 1982

[5] *Deribas, A.A.:* Treatment of Materials by explosive Energy. In: Combustion, Explosion and Shock Waves; September-October, 1987, Volume 23, Issue 5, pp. 639-648

[6] *Kakizaki, S.; Watanabe, M.; Kumai, S.:* Simulation and Experimental Analysis of Metal Jet Emission and Weld Interface Morphology in Impact Welding. In: Materials Transactions - Special Issue on Aluminum Alloys 2010, Vol. 52, No. 5, 2011, pp. 1003-1008

[7] *Johnson, G.R.; Cook, W.H.:* A constitutive model and data for metals subjected to large strains, high strain rates and high temperatures. In: Proceedings of the 7th International Symposium on Ballistics, 1983, pp. 541-547

[8] *Trunov, M. A.; Schoenitz, M.; Dreizin, E. L.:* Ignition of Aluminum Powders Under Different Experimental Conditions. In: Propellants, Explosives, Pyrotechnics, 30, 2005, No. 1, pp. 36-43

[9] *Göbel, G.; Kaspar, J.; Herrmannsdörfer, T.; Brenner, B.; Beyer E.:* Insights into intermetallic phases on pulse welded dissimilar metal joints. In: 4th International Conference on High Speed Forming (ICHSF), 2010